FIRST BEAM TEST RESULT OF A PROTOTYPE WIRE SCANNER FOR THE KEKB INJECTOR LINAC AND BT LINES

Tsuyoshi SUWADA, Naoko IIDA, Yoshihiro FUNAKOSHI, Takashi KAWAMOTO and Mitsuo KIKUCHI
KEK, High Energy Accelerator Research Organization
1-1 Oho, Tsukuba, Ibaraki, 305 Japan

Abstract

The first beam test of a prototype wire scanner for the KEKB injector has been successfully conducted during the machine time of July 7-11 this year. The purpose of the test was to investigate effects of beam background on system performance by using electron beams of the injector linac. This report describes results of the beam test in detail.

1. Introduction

Since the KEKB is a factory machine, a well-controlled operation of its injector is required for minimizing tuning time and a stable operation. For this purpose, beam diagnostic and monitoring tools are essentially important. Of those tools, a wire scanner (WS) system is used to measure transverse beam distributions non-destructively and to determine beam emittances and Twiss parameters which are used in optics matching. To determine these parameters without changing magnet strength, at least 3 WS's are needed in a localized area. For redundancy, we plan to install WS's in sets of four. At 6 critical points of the injector linac and the beam transport (BT) lines, such a set of monitors will be installed. The basic design for the injector linac and BT lines was reported in detail elsewhere[1,2]. The resolution for the beam size measurements is required to be the order of 1%. Empirically performance of the WS is seriously affected by beam background. The main purpose of the beam test was to investigate how serious background is and how we can suppress its effects. We studied effects of beam tuning, detector geometry, detection methods and shield by lead blocks on beam background.

2. Prototype wire scanner and the detection system

A cross-sectional drawing of the prototype WS is shown in Fig. 1. The WS comprises a tungsten wire of 300-μm diameter in a vacuum chamber and a driving unit to drive the wire. The driving unit consists of a pulse motor and precise linear guides. Each of 3 wires meets the others at an angle of 45 degree. Actually the three wires are different parts of a single wire. The wires, which are called H-,V-, and U-wire, go across the beam horizontally, vertically and in the 45-degree direction by driving a wire holder in the direction perpendicular to U-wire. The motion of the wire holder is constrained by two linear guides installed in both sides of the holder along the driving direction. A small port with a polyimide (Kapton) foil of about 76-μm thickness is attached to the vacuum chamber to guide secondary scattered electrons at an angle of 65° with the beam line. Fig. 2 shows a block diagram of the system. The pulse motor is driven with a step resolution of 1μm by a motor driver controlled by a pulse-train generator (PTG, 512Hz). A tuner controller can also drive the pulse motor in a manual mode. The drive position of the wire is monitored by Magnescale with a resolution of 1μm. The driving unit is controlled by a VME/CAMAC system and a host computer through a network. Two types of detection methods were tested in this experiment: one detects γ-rays generated through the bremsstrahlung and another detects secondary electrons scattered at large angles through the Mϕller scattering. For both detection methods, we used photomultipliers (PMs) to which a $30\times30\times10$ mm^3 or $40\times50\times10$ mm^3 plastic scintillator was attached. The PM signals were directly fed to a CAMAC-based charge ADC(LeCroy 2249W) through 15-m-long coaxial cables. A beam timing signal was used to gate the ADC. A control software has been developed based on the EPICS system.[3]

3. Experimental setup

A beam test was performed at the end of the fourth sector of the linac by using electron beams with a pulse width of 1ns in FWHM. The beam energy and beam intensity were 2.7 GeV and 0.2 nC/pulse (5Hz) at the WS. An experimental setup is shown in Fig. 3. Three detectors were placed in the downstream of the WS and at the same level as the beam line. One is an electron detector (e^-) and the other two are photon detectors (γ_1, γ_2), whose detection angles are 65°, 10.2° and 13° with the beam line, respectively. Each detector was sufficiently shielded by using about one-hundred lead blocks against beam background. The detector acceptances were 1.7×10^{-3}, 1.1×10^{-4} and 4.1×10^{-5} sr for the e^-, γ_1 and γ_2 detectors, respectively. Beam intensity of each pulse was measured using a wall-current monitor placed 5m upstream from the WS to make corrections for variations of beam intensity.

4. Beam test procedure

We found that the signal-to-noise (S/N) ratios were very sensitive to beam background. Prior to measurements, sufficient beam tuning was needed to minimize beam loss in the upstream. With a good beam condition, the two detection methods with several detector setup configurations were compared with each other by measuring the S/N ratios. The setup configurations examined are shown in Fig. 4. High voltages (HVs) fed to the PMs were adjusted so as to maximize the S/N ratios within the linear response region of the PMs. The HVs were set to be -800, -800, and -950 V for

e^-, γ_1, and γ_2 detectors, respectively (see Fig.5). Several parameters were tuned by using the beams before the data taking. A drive step length was chosen to be 0.7 mm/step. A whole drive length was set to be 85mm. The number of data points for a scan was 135 points/scan (one data point was constructed by a ten-pulses average). As a result, the total measuring time was about ten minutes for one whole scan including waiting time at each drive step before the start of the data taking to avoid any wire vibration. Fig. 6 shows typical signals using the setup configuration [1-a]. In Fig.4 the measured S/N ratios are shown, which are average values of the data from the three wires. We found that the e^- detection is the best method and that the setup configuration of [1-a] or [2-b] gives the best results. This seems reasonable, since the e^- detector has an advantage of background suppression over the γ detectors. A part of the beam pipe seen directly by the e^- detector is rather smaller than those for the γ detectors. A larger incident angle of background particles to the e^- detector is also contributed to background suppression. On the other hand, the e^- detector with much larger acceptance has comparable signal strength with that of the γ detectors. We changed strength of beam background and investigated its effect for each detection method. Beam background was controlled by changing field strength of a quadrupole magnet located about 39.2m upstream from the WS. The quadrupole strength was changed in a range of ±15% for the nominal strength. The Twiss parameters and emittances were also measured in this method. To investigate the shielding effect of the lead blocks, we intentionally removed some of them for the setup configuration [3-a'] and observed changes of the S/N ratios. This showed that these shield blocks are necessary to suppress beam background.

5. Data analysis and discussions

Fig. 7 shows a comparison of the S/N ratios for the e^- detector to those for the γ (γ_1 and γ_2) detectors. The S/N ratio of the e^- detection is clearly larger than that of the γ detection with the ±15% variation of the quadrupole strength. The data taken with the WS and shown typically in Fig. 6 was fitted with a function which has three peaks and a background. Each peak was assumed to have an asymmetric Gaussian shape and we used an exponential function for the background. We estimated the resolution of the beam size measurement with fitting residuals. Fig. 8 shows a comparison of the beam sizes measured with the e^- detector and the γ detectors. The result shows that the beam sizes obtained with the γ detectors seem to be somewhat larger than those with the e^- detector. The reason is now under investigation. Fig. 9 shows a dependence of the resolution ($\delta\sigma/\sigma(\%)$) of the beam sizes on the S/N ratios. With a good S/N ratio we obtained a resolution of about 3%. This resolution is limited by the drive step length and the number of beam pulses at each step. A better resolution is probably attainable by improving them. Here, we briefly discuss about two systematic error sources: one is the error derived from a finite wire thickness and another is an error in the wire drive. As for the former, the measured beam size σ_m is expressed as $\sigma_m^2 = \sigma_0^2 + \sigma_w^2$, where σ_0 is a true beam size and σ_w is the effective wire thickness dependent on the shape of the cross section. In the case of the round cross section, σ_w is $D/4$. Here, D is a wire diameter and is 300μm for the present wire. Its effect can be corrected in the first order, although the amount of the correction is small in this case. As for the latter, we have to consider wire-positioning errors arising from a winding motion of the wire holder along the driving direction. In this experiment, however, the wire misplacement is small and is estimated to be less than 10μm, since the both sides of the holder are constrained by the linear guides. The emittances were measured using the WS. Results were $\gamma\varepsilon_x = 110\pi$ mm•mrad and $\gamma\varepsilon_y = 82\pi$ mm•mrad which are consistent with those measured using a screen monitor 5m downstream of the WS within the errors.

6. Conclusions

A prototype wire scanner was tested by using electron beams in the injector linac. We found that the e^- detection method at an angle of 65° was better than the γ detection under large beam background. The S/N ratio of the order of 10^2 was obtained after sufficient beam tuning. We obtained the resolution in the beam size measurement of about 3%.

Acknowledgment

The authors gratefully acknowledge S. Yoshida in Kanto Information Service for his help on the software development using EPICS. They also thank to K. Oide for a development of the data analysis tools and H. Koiso for a help in the emittance measurement.. Thanks are also devoted to the KEKB commissioning group who helped the preparation of this experiment.

References

[1] S. Kurokawa, et al., KEK Report 90-24 (1991).
[2] I. Sato, et al., KEK Report 95-18 (1996).
[3] L. R. Dalesio, et al., ICALEPCS 91, KEK Proceedings 92-15 (1992) p.278.

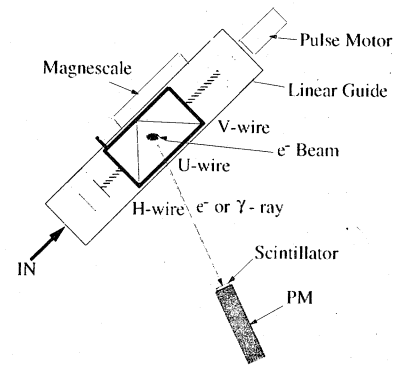

Fig. 1.Cross-sectional drawing of the prototype wire scanner.

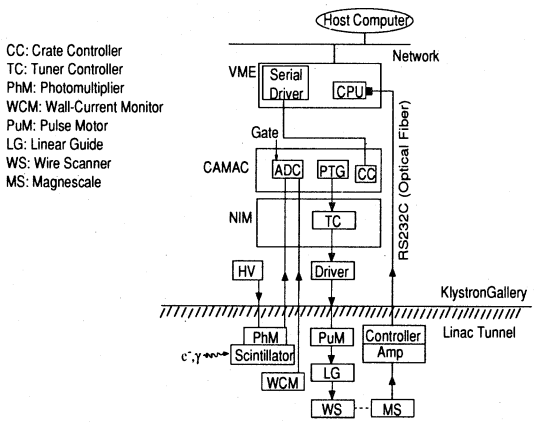

Fig. 2. Block diagram of the system.

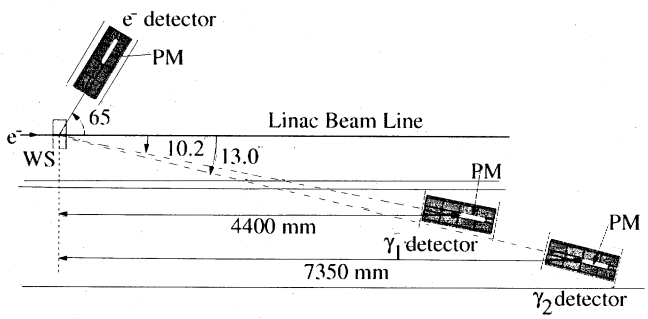

Fig. 3. Experimental setup.

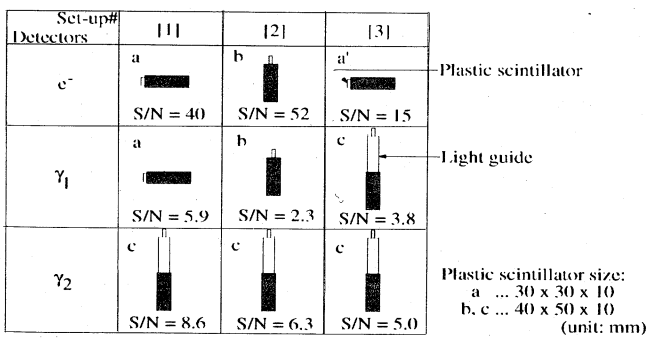

Fig. 4. Detector setup configurations.

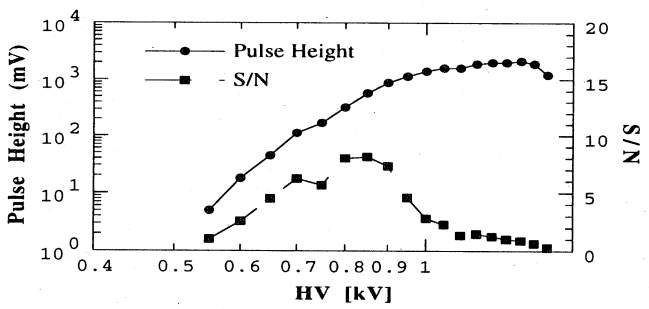

Fig. 5. S/N ratios and signal pulse heights depending on the high voltage fed to the photomultiplier. This figure shows a result for the e^- detector using the setup [1-a].

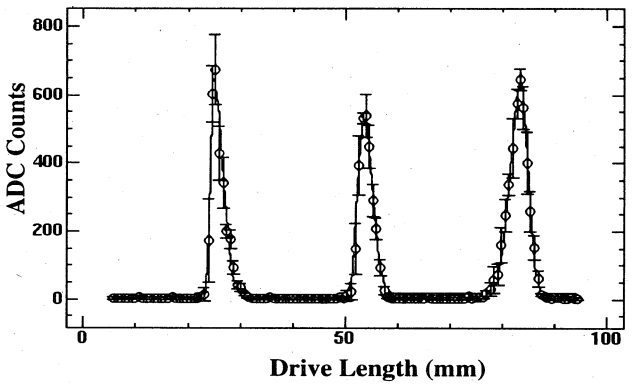

Fig. 6. Typical transverse beam distributions. The left, middle and right peaks correspond to V-, U- and H-wires, respectively.

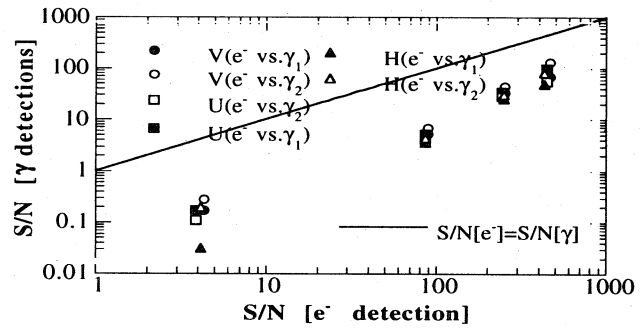

Fig. 7. Correlation plots of the S/N ratios for the e^- detector to those of the γ detectors. A solid line shows a relation of S/N[e^-]=S/N[γ].

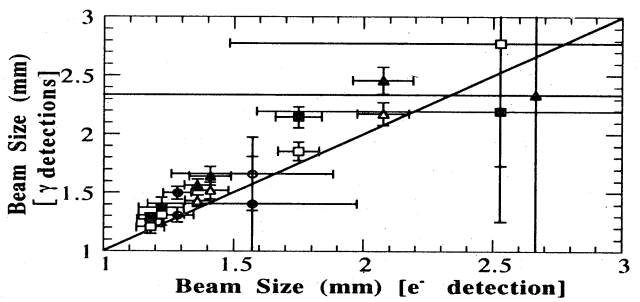

Fig. 8. Variations of the beam sizes(1σ) measured using the e^- detector to those of the γ detectors. The same symbols as in Fig. 7 are plotted. A solid line shows a relation of $\sigma_{e^-} = \sigma_\gamma$.

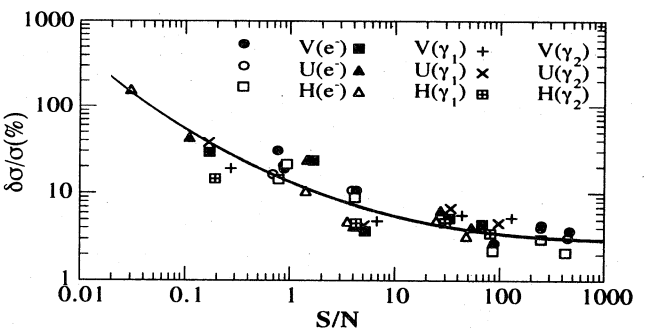

Fig. 9. Resolutions of beam-size measurements dependent on the S/N ratios. A solid line is an eye's guide.